The impact of abrupt suspension of solar radiation management (termination effect) in experiment G2 of the Geoengineering Model Intercomparison Project (GeoMIP)

Andy Jones,[1] Jim M. Haywood,[1,2] Kari Alterskjær,[3] Olivier Boucher,[4] Jason N. S. Cole,[5] Charles L. Curry,[6] Peter J. Irvine,[7] Duoying Ji,[8] Ben Kravitz,[9] Jón Egill Kristjánsson,[3] John C. Moore,[8] Ulrike Niemeier,[10] Alan Robock,[11] Hauke Schmidt,[10] Balwinder Singh,[9] Simone Tilmes,[12] Shingo Watanabe,[13] and Jin-Ho Yoon[9]

[1]   We have examined changes in climate which result from the sudden termination of geoengineering after 50 years of offsetting a 1% per annum increase in CO_2 concentrations by a reduction of solar radiation, as simulated by 11 different climate models in experiment G2 of the Geoengineering Model Intercomparison Project. The models agree on a rapid increase in global-mean temperature following termination accompanied by increases in global-mean precipitation rate and decreases in sea-ice cover. There is no agreement on the impact of geoengineering termination on the rate of change of global-mean plant net primary productivity. There is a considerable degree of consensus for the geographical distribution of temperature change following termination, with faster warming at high latitudes and over land. There is also considerable agreement regarding the distribution of reductions in Arctic sea-ice, but less so for the Antarctic. There is much less agreement regarding the patterns of change in precipitation and net primary productivity, with a greater degree of consensus at higher latitudes.

1. Introduction

[2]   Even under the most optimistic scenarios, greenhouse gas concentrations are predicted to continue to rise into the future leading to significant global warming. Geoengineering via solar radiation management (SRM), i.e., the deliberate brightening of the planet in order to reflect additional sunlight back to space to counteract greenhouse gas induced warming, has been suggested as a plausible countermeasure [e.g., *Mautner*, 1991; *Crutzen*, 2006]. With this in mind, the Geoengineering Model Intercomparison Project (GeoMIP) was established to intercompare results from a wide variety of state-of-the-art coupled atmosphere-ocean general circulation models under specific, nominally identical idealized scenarios [*Kravitz et al.*, 2011]. Geoengineering was simulated either by a reduction of the solar constant in GeoMIP experiments G1 [*Schmidt et al.*, 2012; *Kravitz et al.*, 2013] and G2, or by increasing the concentration of stratospheric aerosols in experiments G3 and G4 to increase the reflection of sunlight away from the Earth.

[3]   One of the issues surrounding geoengineering is that of "moral hazard," the possibility that if large-scale climate engineering is indeed deployed to counteract increases in global temperature, then nothing significant will be done to reduce greenhouse gas emissions as global warming will no longer be perceived as a problem [*Schneider*, 2001; *Robock*, 2008; *Shepherd et al.*, 2009]. If this were to happen then geoengineering efforts would need to be maintained for many years to keep global warming below potentially dangerous levels [*Boucher et al.*, 2009]. The expectation that humankind would be able to continuously maintain a geoengineering effort at the required level for this length of

[1]Met Office Hadley Centre, Exeter, UK.

[2]College of Engineering, Mathematics and Physical Sciences, University of Exeter, Exeter, UK.

[3]Department of Geosciences, University of Oslo, Oslo, Norway.

[4]Laboratoire de Météorologie Dynamique, IPSL, CNRS/UPMC, Paris, France.

[5]Canadian Centre for Climate Modeling and Analysis, Environment Canada, Toronto, Ontario, Canada.

[6]School of Earth and Ocean Sciences, University of Victoria, Victoria, British Columbia, Canada.

[7]Institute for Advanced Sustainability Studies, Potsdam, Germany.

[8]State Key Laboratory of Earth Surface Processes and Resource Ecology, College of Global Change and Earth System Science, Beijing Normal University, Beijing, China.

[9]Atmospheric Sciences and Global Change Division, Pacific Northwest National Laboratory, Richland, Washington, USA.

[10]Max Planck Institute for Meteorology, Hamburg, Germany.

[11]Department of Environmental Sciences, Rutgers, State University of New Jersey, New Brunswick, New Jersey, USA.

[12]National Center for Atmospheric Research, Boulder, Colorado, USA.

[13]Japan Agency for Marine-Earth Science and Technology, Yokohama, Japan.

Corresponding author: A. Jones, Met Office Hadley Centre, Fitzroy Road, Exeter, EX1 3PB, UK. (andy.jones@metoffice.gov.uk)
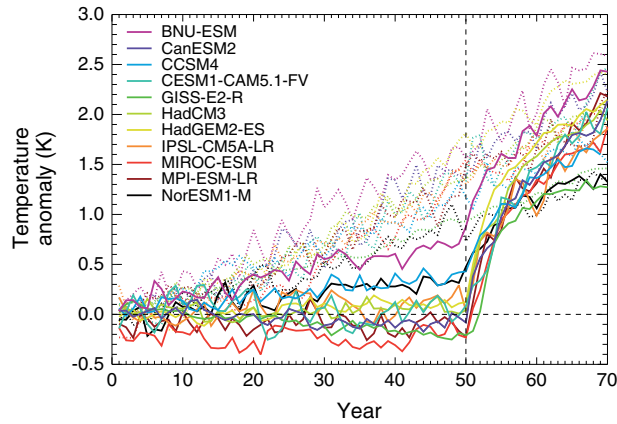
Figure 1. Evolution of annual mean anomaly of global mean near-surface air temperature (K) in the G2 simulations (solid lines) with respect to the long-term mean from each model's CMIP5 piControl simulation. Time series from corresponding 1pctCO2 simulations are also shown (dotted lines). The termination of geoengineering in the G2 simulations is indicated by the dashed vertical line.

time is questionable, to say the least. It therefore appears relevant to investigate the so-called "termination effect": what might be the climatic impacts of a sudden termination of geoengineering after a number of years during which it was used to counterbalance greenhouse gas increases? The rate of climate change is important because the ability of ecosystems to respond can be compromised if the changes are too rapid [e.g., *Davis and Shaw*, 2001].

[4] The effects of sudden changes in forcing have been studied previously for both increases [e.g., *Geoffroy et al.*, 2013] and decreases [e.g., *Held et al.*, 2010] in greenhouse gas forcing. It has also been studied in specific geoengineering contexts using individual models [*Wigley*, 2006; *Matthews and Caldeira*, 2007; *Robock et al.*, 2008; *Brovkin et al.*, 2009; *Irvine et al.*, 2012]. All these studies found a rapid response to sudden changes in forcing, with global-mean temperatures responding to the new forcing levels within 5 years or so. Here we use a common experimental design to compare the responses of different climate models to the termination of geoengineering in an idealized scenario, described below. These are not in any way projections of what might happen under specific climate/geoengineering conditions, but rather an examination of the level of agreement between current climate models in an idealized termination scenario. Of course, other more or less extreme scenarios could be examined, but the rationale of studying such scenarios would be the same: to assess the robustness of model responses by identifying the degree of inter-model similarity under a particular scenario.

2. Modeling Framework

[5] We have analyzed the termination effect in GeoMIP experiment G2 [*Kravitz et al.*, 2011] using data provided by 11 different modeling groups (see Table 1 in *Kravitz et al.* [2013] for details of the models). GeoMIP experiment G2 is parallel to the CMIP5 simulation known as

1pctCO2 (1% CO_2 rise per annum from preindustrial levels; *Taylor et al.* [2012]) and attempts to counteract the increasing CO_2 concentration by a gradual reduction of the solar constant, calculated as follows. The reduction of the solar constant required to counteract a quadrupling of CO_2 from preindustrial levels, ΔS_c, had previously been evaluated for each model for GeoMIP experiment G1 [*Kravitz et al.*, 2013]. This was done by ensuring that the top-of-atmosphere (ToA) net radiation over the first 10 years of a simulation with $4 \times CO_2$ levels and reduced solar constant was within 0.1 W m^{-2} of that of each model's CMIP5 preindustrial control (piControl) simulation. The logarithmic dependence of radiative forcing on CO_2 concentration means that forcing increases in an approximately linear manner during 1pctCO2. Given that a 1% increase of CO_2 per annum reaches $4 \times CO_2$ after $\sim$140 years, the value of ΔS_c calculated for G1 can be used to construct a linear rate of decrease of the solar constant to offset a 1% per annum CO_2 increase. Note that the forcing from ΔS_c may not be identical (but of opposite sign) to that due to $4 \times CO_2$ as the efficacy of solar forcing may not be unity [*Hansen et al.*, 2005]: *Schmidt et al.* [2012] found a mean solar efficacy of 0.78 for four of the models participating in the present study. The rate of decrease of the solar constant may be refined if necessary to ensure that, as with experiment G1, the ToA net radiation over the first 10 years of G2 was within 0.1 W m^{-2} of each model's piControl.

[6] Geoengineering was terminated after 50 years and the simulations continued for a further 20 years. It should be noted that both 1pctCO2 and G2 are highly idealized simulations and not actual climate change projections. Nevertheless, they are useful tools in examining the responses of a range of different climate models to geoengineering and its termination.

3. Results

3.1. Global-Mean Changes

[7] Figure 1 shows the evolution of global-mean near-surface air temperature anomalies from the various G2 simulations (solid lines) and their corresponding 1pctCO2 simulations (dotted lines). Anomalies are calculated against

Table 1. Residual Differences in Global-Mean Near-Surface Air Temperature ($\Delta(T)$, K) and Precipitation Rate ($\Delta(pr)$, mm d^{-1}) Between G2 and 1pctCO2 Simulations Over the Final Decade (Years 61–70) of the G2 Experiment (G2 Minus 1pctCO2)[a]

Model	$\Delta(T)$	$\Delta(pr)$	$\Delta(T_{1pctCO2})$
BNU-ESM	−0.24	**−0.004**	2.43
CanESM2	−0.37	−0.024	2.13
CCSM4	−0.09	−0.008	1.63
CESM-CAM5.1-FV	−0.28	−0.018	2.06
GISS-E2-R	−0.11	−0.009	1.37
HadCM3	−0.13	−0.010	1.97
HadGEM2-ES	−0.35	−0.022	2.31
IPSL-CM5A-LR	−0.25	−0.022	1.85
MIROC-ESM	−0.31	−0.022	1.90
MPI-ESM-LR	**-0.01**	−0.004	1.83
NorESM1-M	**+0.05**	**+0.001**	1.26

[a]Differences which are not statistically significant at the 5% level are shown in **bold**. Also given ($\Delta(T_{1pctCO2})$, K) is the mean warming in 1pctCO2 for years 61–70 compared with piControl for each model.
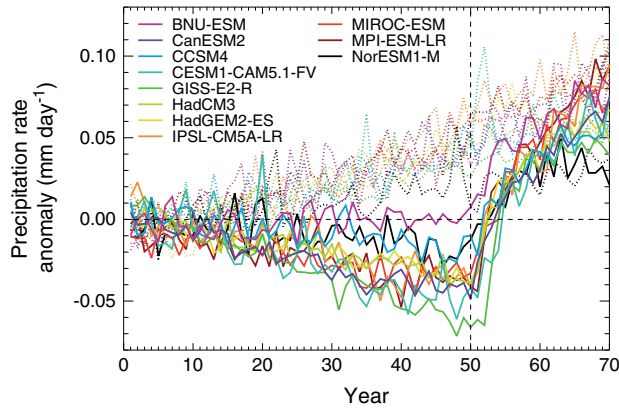
Figure 2. As in Figure 1 but for the anomaly in global mean precipitation rate (mm d^{-1}).

Figure 3. As in Figure 1 but for the anomaly in global mean land vegetation net primary productivity (Pg[C] yr^{-1}).

the long-term mean of each model's CMIP5 piControl simulation. It is clear that the different models have maintained global-mean temperatures near preindustrial levels during the geoengineering phase with varying degrees of success. The multimodel mean temperature anomaly in G2 at year 50 is 0.12 ± 0.35 K, over a degree cooler than the mean anomaly in 1pctCO2 (1.33 ± 0.30 K). Understanding why certain models have greater or lesser amounts of warming would require detailed analysis of the models in question, which is beyond the scope of this study.

[8] Of more relevance here is that when geoengineering is terminated, all models warm rapidly, tending toward their respective 1pctCO2 temperatures at broadly similar rates (mean e-folding time is 6.3 ± 2.0 years, calculated from linear fits to the natural logarithm of G2 anomalies with respect to 1pctCO2). This rate of change is similar to those found previously, e.g., *Geoffroy et al.* [2013] found a mean fast-response relaxation time of 4.1 years when examining the response to an instantaneous $4 \times CO_2$ change in 16 CMIP5 models. Most of the G2 simulations do not quite reach their respective 1pctCO2 temperatures within the period of the G2 experiment due to reduced ocean heat uptake during 50 years of geoengineering. The residual temperature differences averaged over the final decade of the experiment are given in Table 1.

[9] Figure 2 shows the evolution of global-mean precipitation rate. All models except one show varying degrees of reduction in precipitation rate during the geoengineering period, again followed by a rapid increase on termination. The one model in which global-mean precipitation is roughly constant during the geoengineering period (BNU-ESM) is the one which shows the greatest degree of warming during this period, a demonstration of how global SRM cannot maintain both global-mean temperature and precipitation simultaneously [e.g., *Ban-Weiss and Caldeira*, 2010]. As with near-surface temperature, global-mean precipitation rate in the majority of G2 simulations does not quite recover to 1pctCO2 levels within the period covered by this experiment (Table 1).

[10] Figure 3 shows the evolution in land net primary productivity (NPP), a measure of the flux of carbon to (or from) land-based vegetation (note that HadCM3 does not simulate this quantity). There is a much larger range of NPP from the different models compared with temperature or
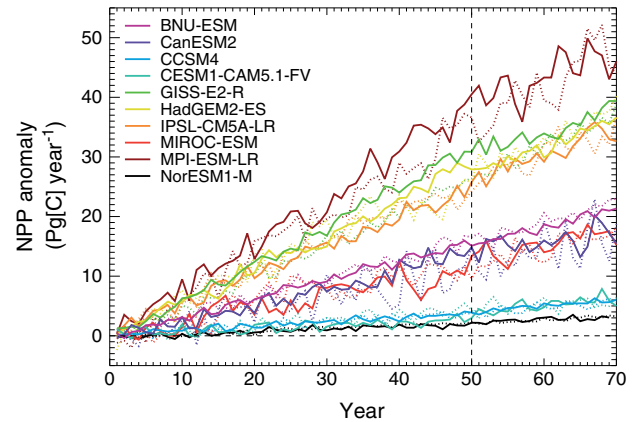
precipitation, reflecting the different parameterizations (or implementations thereof) in each model. As photosynthesis is enhanced by higher CO_2 levels, the changes in global-mean NPP are dominated by the steady rise in CO_2 throughout both 1pctCO2 and G2 simulations. An examination of the linear trends in global-mean NPP before and after geoengineering termination reveals no agreement between the models on the impact of termination. Five models show no significant alteration in the rate of change of NPP (at the 5% significance level), and of the five which do show a significant change, four exhibit a slowdown in the rate of NPP increase while one has an acceleration.
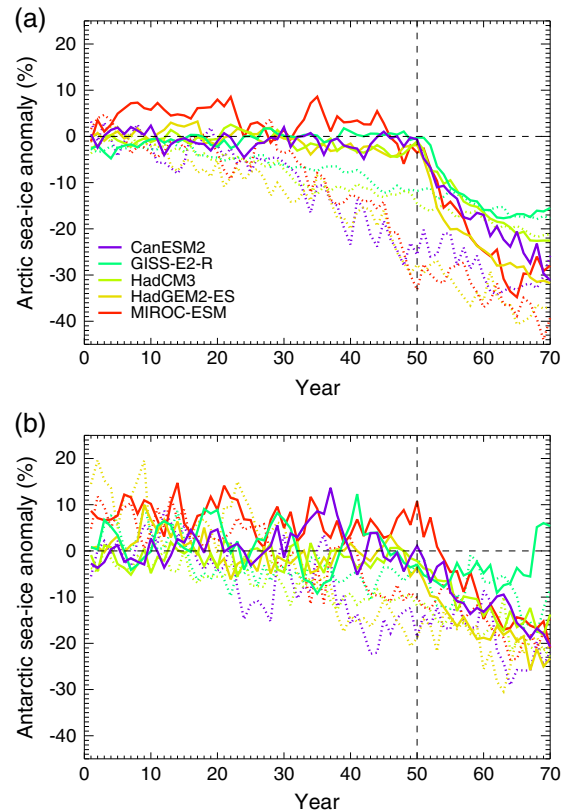

Figure 4. As in Figure 1 but for the anomaly in (a) Arctic and (b) Antarctic sea-ice area (%).
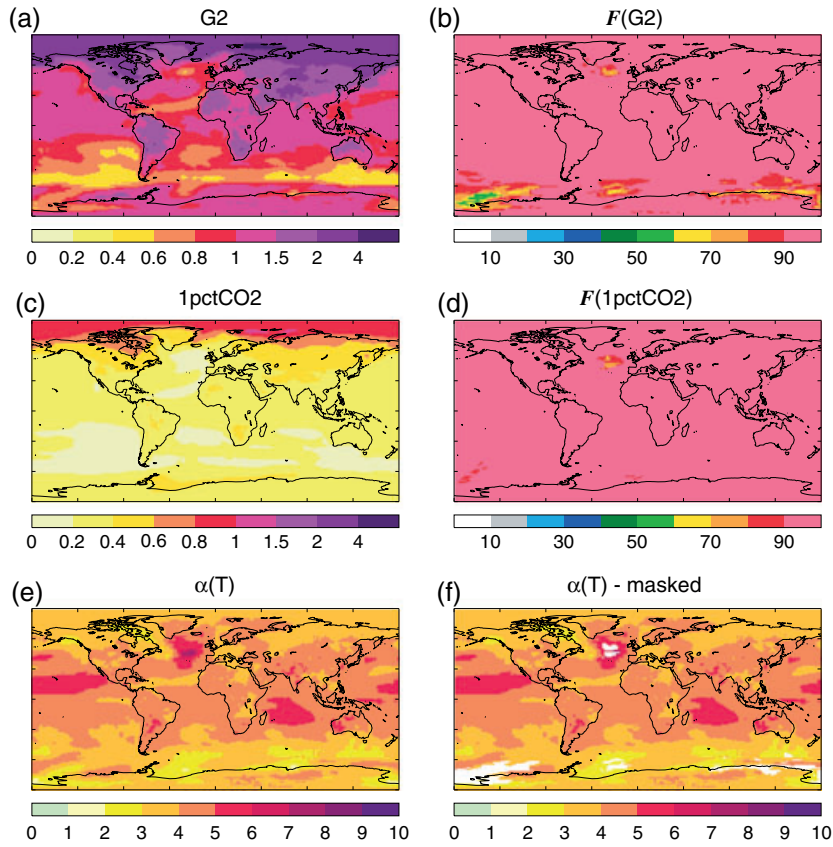
Figure 5. (a) Multimodel mean rate of change of annual-mean near-surface air temperature (K per decade) in G2 over the decade immediately following termination of geoengineering. (b) The proportion F (%) of models which agree with the sign of the change in Figure 5a. (c) As in Figure 5a but for the first 70 years of 1pctCO2. (d) As in Figure 5b but for 1pctCO2. (e) The ratio of Figures 5a and 5c, i.e., a distribution of $\alpha(T)$ (no unit). Values >1 indicate a more rapid change in G2 than in 1pctCO2, values <1 slower changes. (f) As in Figures 5e but masked to only show those areas where >75% of models agree on the sign of the changes in both G2 and 1pctCO2.

[11] The evolution of Arctic and Antarctic sea-ice areas are shown in Figure 4 (only data from the five models indicated are included due to technical difficulties in analyzing the sea-ice data from the other models). In the Arctic, there is considerable difference between the models as to the rate of sea-ice loss in the 1pctCO2 simulations, whereas the models are rather more consistent in the Antarctic. During the geoengineering phase of G2, both Arctic and Antarctic sea-ice amounts are roughly constant compared with the decline in 1pctCO2. This is consistent with the mean rate of polar warming being between ~10 (Arctic) and ~8 (Antarctic) times slower during geoengineering in G2 compared with 1pctCO2 for these models. Changes in Antarctic sea-ice are generally smaller than those in the Arctic, both in 1pctCO2 and in G2 following termination. Once geoengineering is terminated, all models show a rapid decline in sea-ice toward the levels of the 1pctCO2 simulations, although there is a great deal of variability evident in the GISS-E2-R model in the Antarctic.

3.2. Quantifying the Termination Effect

[12] A simple approach to quantifying the termination effect is to calculate for each model a nondimensional "termination acceleration factor" (α). For global-mean near-surface air temperature T, we define $\alpha(T)$ as the mean rate of change in G2 during the decade immediately following geoengineering termination normalized by the mean rate of change over the whole 1pctCO2 simulation; rates of change are calculated using simple linear regression. $\alpha(T)$ is therefore a measure of how much faster the planet warms following termination compared with the warming due to a 1% CO_2 rise per annum. Its absolute value is a function of the scenario being considered and the date of geoengineering termination, so $\alpha(T)$ should only be used as a means to compare model results within a specific context. As defined, α is only applicable for experiments where the control simulation has a simple, broadly monotonic increase in net forcing, such as the 1pctCO2 simulation used as the control for G2. Alternative definitions of α could be devised using different time periods or fitting methods (the changes in the termination phase are obviously not linear), but for the purposes of intercomparison between different models in the same experiment, we consider the simple approach taken here to be adequate. Similar termination acceleration factors can be determined for global-mean precipitation rate ($\alpha(pr)$), net primary productivity ($\alpha(NPP)$), and sea-ice cover ($\alpha(SIC)$). Values of α from the G2 models are given in Tables 2 and 3.
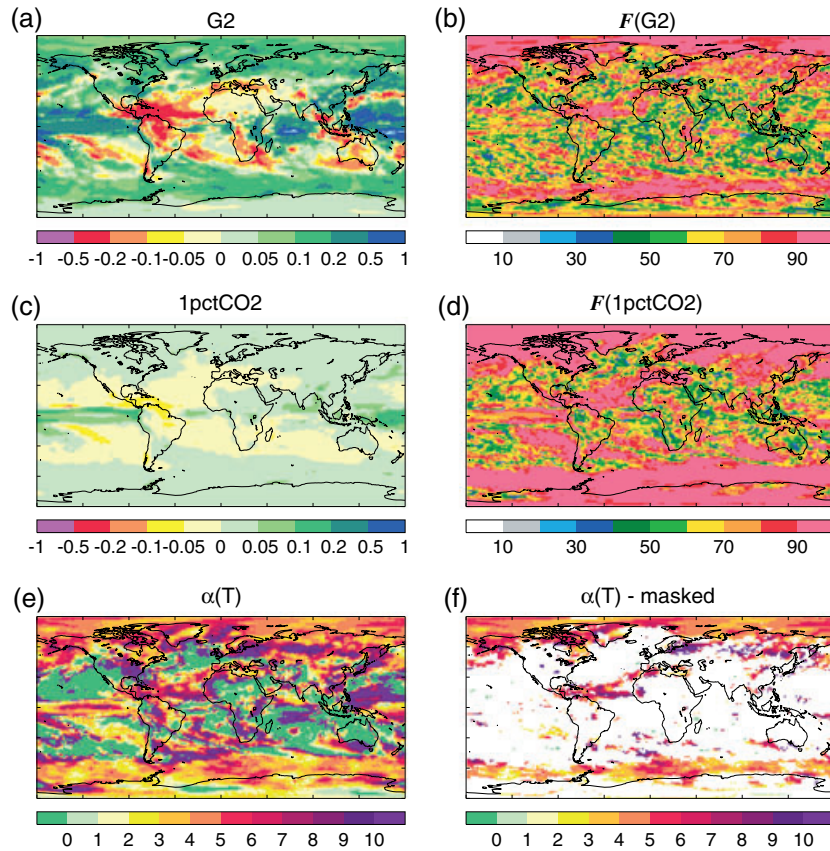
Figure 6. (a)–(d) As in Figure 5 but for the rate of change of annual-mean precipitation rate (mm day^{-1} per decade). (e) As in Figure 5 but also including negative values which indicate areas where the changes in G2 and 1pctCO2 are of opposite sign. (f) As in Figure 5.

[13] There is clearly a wide range of α across the models, but all indicate a significant post-termination increase in the rate of warming (mean acceleration factor of 4.1) and global-mean precipitation rate (mean acceleration factor of 6.9) compared with the 1% CO_2 per annum scenario. It should be borne in mind that the amplitude of forcing the models are responding to at termination depends on the amount the solar constant was reduced in each model to counteract CO_2 increases and so is not identical across models. The models are in closer agreement regarding the acceleration factor for temperature (one standard deviation of $\alpha(T)$ being ∼30% of the mean value; see Table 2) than for precipitation (one standard deviation is ∼45% of the mean).

[14] In contrast, differing behaviors among the models are indicated by the range of values for $\alpha(NPP)$. Seven of the models show values of $\alpha(NPP)$ which are <1, indicating a slowing of the rate of increase of NPP when geoengineering is terminated. This is consistent with a negative impact on plant growth of the rapid warming following termination. However, three models have $\alpha(NPP)$ >1, indicating an acceleration in NPP growth. One of these models (CCSM4) is the model that was found to have a statistically significant increase in the rate of global-mean NPP growth in section 3.1. The models which exhibit this behavior are the only ones in this comparison which include a treatment of the nitrogen cycle, in which nitrogen deposition is kept constant at 1850 levels in both 1pctCO2 and G2 simulations. The acceleration of NPP is a fertilization effect [*Thornton*

et al., 2009], caused by the liberation of nitrogen brought about by the increased rates of microbial decomposition in soils as the climate warms following geoengineering termination. However, as shown in Figure 3, there is very little difference between each model's G2 and 1pctCO2 simulations, so this result may not be robust: of the three models with a nitrogen cycle, only one showed a statistically significant change (increase) in global-mean NPP following termination. The inclusion of the nitrogen-carbon cycle

Table 2. Nondimensional Termination Acceleration Factors for Global-Mean Near-Surface Air Temperature ($\alpha(T)$), Precipitation Rate ($\alpha(pr)$) and Land NPP ($\alpha(NPP)$) for Each Model[a]

Model	$\alpha(T)$	$\alpha(pr)$	$\alpha(NPP)$
BNU-ESM	2.40	3.98	0.95
CanESM2	3.92	5.30	0.28
CCSM4	3.54	6.29	1.77
CESM-CAM5.1-FV	4.30	6.91	1.67
GISS-E2-R	7.00	15.12	0.42
HadCM3	4.63	8.49	–
HadGEM2-ES	3.60	4.79	0.67
IPSL-CM5A-LR	3.34	4.75	0.84
MIROC-ESM	4.55	4.96	0.47
MPI-ESM-LR	4.95	6.93	0.17
NorESM1-M	3.31	7.99	1.58
Mean	4.1 ± 1.2	6.9 ± 3.1	0.88 ± 0.60

[a]The mean is given ± one standard deviation.

Table 3. Nondimensional Termination Acceleration Factors for the Loss of Arctic and Antarctic Sea-Ice Cover (α(SIC))[a]

Model	α(SIC)$_{Arctic}$	α(SIC)$_{Antarctic}$
CanESM2	2.93	3.68
GISS-E2-R	6.85	−0.65
HadCM3	4.62	3.89
HadGEM2-ES	3.50	2.42
MIROC-ESM	3.43	4.87
Mean	4.3 ± 1.6	2.8 ± 2.1

[a]The mean is given ± one standard deviation.

interaction in these models also reduces the CO_2 sequestered in land ecosystems and hence absolute levels of NPP [*Thornton et al.*, 2009]. These three models exhibit the lowest increase in global-mean NPP (Figure 3) because the inclusion of the nitrogen cycle leads to a lower rate of carbon uptake with increasing levels of CO_2 compared with models which do not simulate the nitrogen cycle.

[15] The values of α(SIC) given in Table 3 show only a limited degree of agreement among the models considered. All show an increase in the rate of Arctic sea-ice loss, consistent with the rapid warming in the termination phase. Antarctic sea-ice also shows an increased rate of decline in four of the models analyzed, and whilst the remaining model (GISS-E2-R) actually shows a small increase in sea-ice compared with 1pctCO2 (α(SIC) < 0), although an examination of Figure 4 indicates that this is best interpreted as "little change". There is no agreement as to whether acceleration of sea-ice change is greatest in the Arctic or in the Antarctic following geoengineering termination.

3.3. Geographical Variations

[16] In addition to considering the rate of global-mean change following termination, it is also important to consider the geographical distribution of such changes. The impacts of regional changes in temperature, precipitation, NPP, and sea-ice are of more relevance than global-mean changes to natural ecosystems and to the response of human societies, such as the amount of adaptation required to respond to termination-induced changes.

[17] Figure 5a shows the multimodel average of the mean rate of change of near-surface temperature in G2 over the decade immediately following geoengineering termination, calculated from a linear fit at each point. Figure 5b shows the proportion F (%) of models which agree with the sign of the change shown in Figure 5a, indicating a high degree of agreement among the models. Figures 5c and 5d show similar plots for the mean temperature change in 1pctCO2. Note that the absolute values of the rates of change are not particularly meaningful as they relate to idealized simulations: it is the comparative differences between the rates in different regions and the amount of agreement among the model which is important. How these results might relate to changes under more realistic scenarios depends on the linearity of the responses to the imposed forcing.
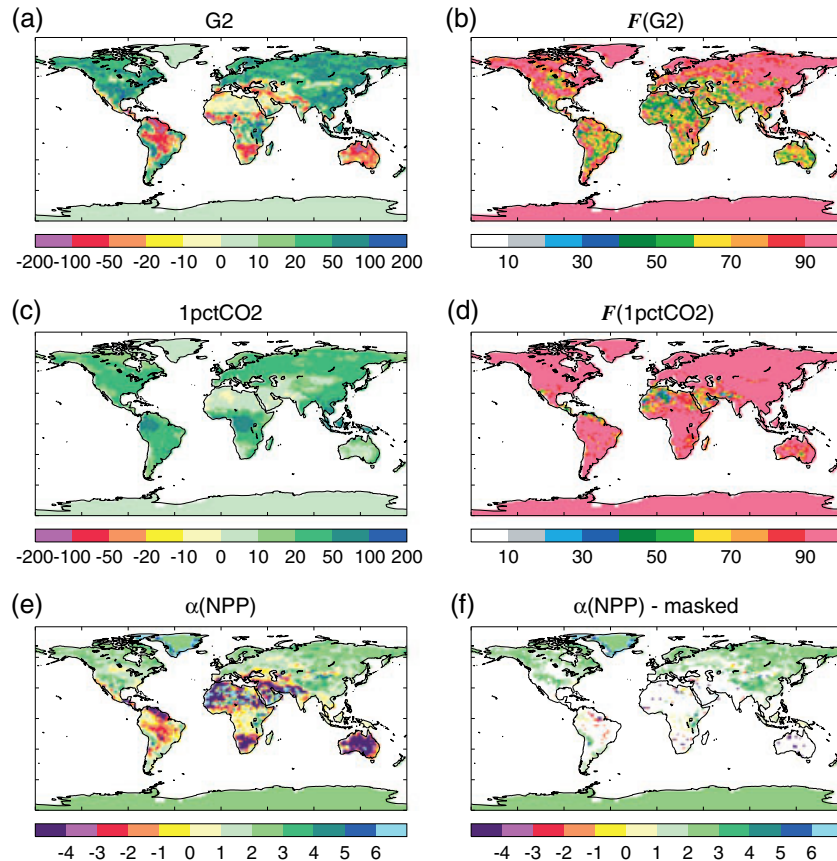
Figure 7. As in Figure 6 but for the rate of change of terrestrial net primary productivity (g[C] m^{-2} yr^{-1} per decade).
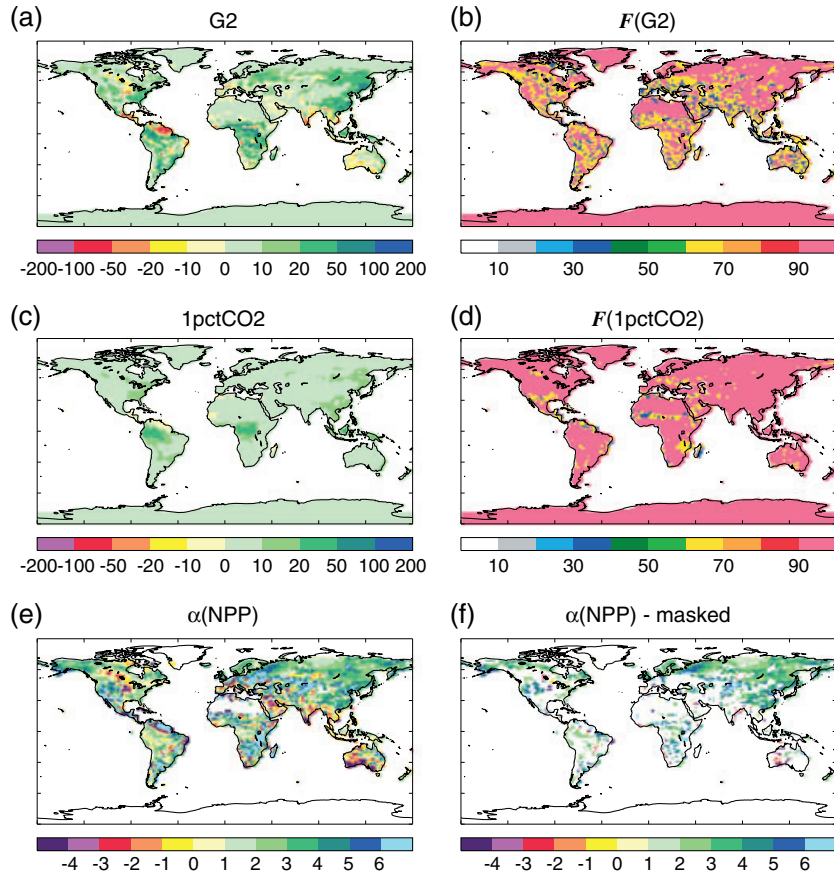
Figure 8. As in Figure 7 but only for the three models which include a treatment of the nitrogen cycle (CCSM4, CESM1-CAM5.1-FV, and NorESM1-M).

[18] Both Figures 5a and 5c indicate higher warming rates over land compared with ocean areas, as expected from the higher heat capacity of the oceans. These figures also indicate faster warming in the Northern Hemisphere compared with the Southern, with the highest rate of warming over the Arctic with a maximum in the Barents Sea. For comparison, the observed rate of warming of the Arctic has been up to $\sim$0.4 K/decade over the last several decades [*Chapin et al.*, 2005], while the mean rate of change predicted by the models is $\sim$0.7 K/decade in 1pctCO2 compared with $\sim$2.4 K/decade in G2 after termination of geoengineering. While the greatest warming is at high latitudes and over land in both G2 and 1pctCO2, Figures 5e and 5f show that the greatest acceleration of warming after geoengineering termination tends to be at lower latitudes and over oceans.

[19] The rate of change of precipitation rate, calculated in the same manner as for temperature, is shown in Figure 6. It is evident that there is much less intermodel agreement regarding precipitation changes than there is for changes in temperature. There is, however, a degree of consensus for precipitation rate increases after termination in G2 at mid-latitude to high latitude (Figure 6b), which are areas where there is a large suppression of precipitation under SRM geoengineering [*Schmidt et al.*, 2012]. There are also indications of agreement on precipitation reduction in G2 in the areas around the Caribbean, the Mediterranean and the north of South America. The patterns of increase and decrease in G2 (Figure 6a) are also seen in 1pctCO2 (Figure 6c) but at a

much slower rate, as indicated by the distribution of $\alpha(pr)$ shown in Figures 6e and 6f. The areas where the majority of models agree on the sign of precipitation changes in G2 (Figure 6b) are broadly the same as those in 1pctCO2 (Figure 6d), suggesting that the intermodel differences are not scenario-dependent. The pattern of precipitation changes seen here is also found in modeling studies of a quadrupling of CO_2 concentrations from preindustrial levels [*Schmidt et al.*, 2012].

[20] Note that Figure 6e shows areas where $\alpha(pr)$ is negative, indicating that the multimodel mean precipitation changes in G2 and 1pctCO2 are of different signs in these areas (which are not, however, regions of model agreement). Negative values of α (for whichever variable) highlight areas where the response to termination may be qualitatively different to that under 1pctCO2 and not simply a scaled version of the same response. This is especially the case for NPP as described below.

[21] The multimodel mean of the rate of change of NPP over the termination phase of G2 is shown in Figure 7a. Over most of the land surface north of about 30°N Figure 7b indicates that the models agree on an increase in NPP as the vegetation responds to warmer conditions in a high-CO_2 environment. In contrast, at lower latitudes, there are indications of a reduction of NPP in areas such as the north of South America and around the Mediterranean, probably related to both reduction in precipitation and rapid warming in areas which may already be heat-stressed. However,

it is clear from Figure 7b that there are also large areas of disagreement among the models at low latitudes. The response in 1pctCO2 is shown in Figures 7c and 7d and shows a general agreement among models for increases in NPP over almost all land areas in this scenario. At high latitudes, NPP increases more slowly in 1pctCO2 than in the termination phase of G2, whereas at low latitudes, 1pctCO2 still shows positive rates of change of NPP in areas where G2 has negative changes (Figures 7e and 7f). Given that the rate of near-surface temperature increase at low latitudes is 3–5 times larger in the termination phase of G2 compared with 1pctCO2, this is perhaps not surprising. Figure 8 shows the results when only considering the three models which include a treatment of the nitrogen cycle. As expected from the global-mean results, these show much lower rates of change of NPP in both G2 and 1pctCO2 (Figures 8a and 8c) and also more areas of positive α(NPP) when compared with Figure 7. Even these three models do not agree, however, on the sign of the change in NPP following termination in many areas (Figure 8b).

[22] Figures 9a and 10a show the multimodel mean rates of change of Arctic and Antarctic sea-ice cover, respectively, during the termination phase of G2 using the models listed in Table 3. There is more agreement for changes in the Arctic compared with the Antarctic (Figures 9b and 10b), with areas of disagreement in the Arctic largely restricted to the
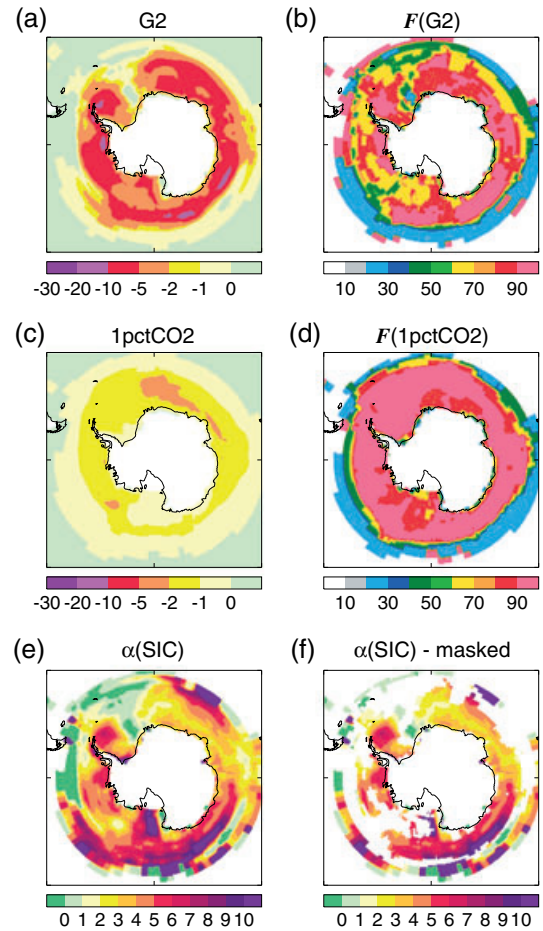

Figure 10. As in Figure 9 but for Antarctica.

periphery of the sea-ice. This is also seen in the Antarctic, but there are also areas of disagreement which extend right to the coast in the east of the Weddell Sea (east of the Antarctic Peninsula) and also from the Ross to the Amundsen Seas (lower left quadrant in Figure 10b). For the 1pctCO2 simulations, the changes are slower and there is general agreement between the models for Antarctic changes (Figure 10d). Figures 9e and 9f indicate that the greatest accelerations of sea-ice loss in the Arctic basin are at lower latitudes (e.g., the Sea of Okhotsk) and in the Barents Sea. For Antarctica, Figures 10e and 10f suggests accelerated sea-ice loss both toward the periphery of the ice and also closer to the coast, e.g., around the Antarctic Peninsula.

4. Discussion

[23] As well as the temperature difference between geoengineered and nongeoengineered simulations at the point of termination, the subsequent rate of temperature increase would also depend on how rapidly geoengineering was terminated. This study has concentrated on the effects of an uncontrolled termination of geoengineering, but it might be argued that termination as simulated in experiment G2 is too rapid as it takes the form of an instantaneous increase of the solar constant back to its unmodified value. In contrast, GeoMIP experiment G4 [*Kravitz et al.*, 2011] simulates SRM by the possibly more realistic mechanism of

Figure 9. As in Figure 6 but for the rate of change of annual-mean Arctic sea-ice area (% per decade).

stratospheric aerosol injection, and an uncontrolled termination of geoengineering in this scenario would cause the ToA net radiation budget to change more slowly as it takes 1 to 2 years for stratospheric aerosol loadings to reduce. An examination of the G2 and G4 simulations of the HadGEM2-ES model shows that the global-mean temperature differences between geoengineered and nongeoengineered simulations at the point of termination are fairly similar in the two experiments (∼1.6 K in G2 and ∼1.2 K in G4), and comparing the rate of change of near-surface air temperature in the termination phases of the experiments shows that warming is indeed faster in G2 than in G4. However, the difference is not large: temperatures in the geoengineered simulations return to nongeoengineered levels with e-folding times of 6.4 and 8.3 years for G2 and G4, respectively. This suggests that the manner in which an uncontrolled termination of geoengineering is simulated in experiment G2 is adequate.

5.   Conclusions

[24]   All the models participating in this GeoMIP experiment agree that significant climate change would ensue rapidly upon the termination of geoengineering, with temperature, precipitation, and sea-ice cover very likely changing considerably faster than would be experienced under the influence of rising greenhouse gas concentrations in the absence of geoengineering. The absolute rate of change would depend on how long solar-reduction geoengineering had been employed, its efficiency at reducing the warming due to greenhouse gas increases, and the rate of greenhouse gas emissions—in short, on the amount of greenhouse gas radiative forcing that geoengineering was offsetting at the time of termination.

[25]   There is fairly good agreement between the models regarding the patterns of warming following termination of geoengineering, and also on the patterns of reduction in sea-ice, especially in the Arctic. However, there is far less of a consensus regarding the regional changes in precipitation and NPP. The distribution of changes in temperature following termination is likely to be similar to that experienced under nongeoengineered climate change but occurring much faster. Although the changes in precipitation distribution on termination appear, as with the warming, basically to be a reversion to the situation which would have existed in a nongeoengineered world, the fact that some regions would experience a reduction in precipitation in addition to rapid warming could stress such regions even further, as suggested by the changes in NPP.

References

Ban-Weiss, G. A., and K. Caldeira (2010), Geoengineering as an optimization problem, *Environ. Res. Lett.*, *5*(034009), doi:10.1088/1748-9326/5/3/034009.

Boucher, O., J. A. Lowe, and C. D. Jones (2009), Implications of delayed actions in addressing carbon dioxide emission reduction in the context of geo-engineering, *Clim. Change*, *92*, 261–273, doi:10.1007/s10584-008-9489-7.

Brovkin, V., V. Petoukhov, M. Claussen, E. Bauer, D. Archer, and C. Jaeger (2009), Geoengineering climate by stratospheric sulfur injections: Earth system vulnerability to technological failure, *Clim. Change*, *92*, 243–259, doi:10.1007/s10584-008-9490-1.

Chapin, F. S., III et al. (2005), Role of land-surface changes in Arctic summer warming, *Science*, *310*, 657–660, doi:10.1126/science.1.117368.

Crutzen, P. (2006), Albedo enhancement by stratospheric sulfur injections: A contribution to resolve a policy dilemma *Clim. Change*, *77*, 211–220, doi:10.1007/s10584-006-9101-y.

Davis, M. B., and R. G. Shaw (2001), Range shifts and adaptive responses to Quaternary climate change, *Science*, *292*, 673–679.

Geoffroy, O., D. Saint-Martin, D. J. L. Olivié, A. Voldoire, G. Bellon, and S. Tytéca (2013), Transient climate response in a two-layer energy-balance model. Part I: Analytical solution and parameter calibration using CMIP5 AOGCM experiments, *J. Clim.*, *26*, 1841–1857, doi:10.1175/JCLI-D-12-00195.1.

Hansen, J., et al. (2005), Efficacy of climate forcings, *J. Geophys. Res.*, *110*, D18104, doi:10.1029/2005JD005776.

Held, I. M., M. Winton, K. Takahashi, T. Delworth, F. Zeng, and G. K. Vallis (2010), Probing the fast and slow components of global warming by returning abruptly to preindustrial forcing, *J. Clim.*, *23*, 2418–2427, doi:10.1175/2009JCLI3466.1.

Irvine, P. J., R. L. Sriver, and K. Keller (2012), Tension between reducing sea-level rise and global warming through solar-radiation management, *Nature Clim. Change*, *2*, 97–100, doi:10.1038/nclimate1351.

Kravitz, B., A. Robock, O. Boucher, H. Schmidt, K. Taylor, G. Stenchikov, and M. Schulz (2011), The Geoengineering Model Intercomparison Project (GeoMIP), *Atmos. Sci. Lett.*, *12*, 162–167, doi:10.1002/asl.316.

Kravitz, B., et al. (2013), Climate model response from the Geoengineering Model Intercomparison Project (GeoMIP), *J. Geophys. Res. Atmos.*, *118*, doi:10.1002/jgrd.50646.

Matthews, H. D., and K. Caldeira (2007), Transient climate-carbon simulations of planetary geoengineering, *Proc. Natl. Acad. Sci. U.S.A.*, *104*, 9949–9954, doi:10.1073/pnas.0700.419104.

Mautner, M. (1991), A space-based screen against climate warming, *J. Brit. Interplan. Soc.*, *44*, 135–138.

Robock, A. (2008), 20 reasons why geoengineering may be a bad idea, *Bull. Atomic Scientists*, *64*(2), 14-18, 59, doi:10.2968/064.002006.

Robock, A., L. Oman, and G. Stenchikov (2008), Regional climate responses to geoengineering with tropical and Arctic SO_2 injections, *J. Geophys. Res.*, *113*, D16101, doi:10.1029/2008JD010050.

Schmidt, H., et al. (2012), Solar irradiance reduction to counteract radiative forcing from a quadrupling of CO_2: Climate responses simulated by four Earth system models, *Earth Syst. Dynam.*, *3*, 63–78, doi:10.5194/esd-3-63-2012.

Schneider, S. H. (2001), Earth systems engineering and management, *Nature*, *409*, 417–421, doi:10.1038/35.053203.

Shepherd, J., et al. (2009), *Geoengineering the Climate: Science, Governance and Uncertainty, The Royal Society*, UK, London.

Taylor, K. E., R. J. Stouffer, and G. A. Meehl (2012), An overview of CMIP5 and the experiment design, *Bull. Amer. Met. Soc.*, *93*, 485–498, doi:10.1175/BAMS-D-11-00094.1.

Thornton, P. E., S. C. Doney, K. Lindsay, J. K. Moore, N. Mahowald, J. T. Randerson, I. Fung, J.-F. Lamarque, J. J. Fedema, and Y.-H. Lee (2009), Carbon-nitrogen interactions regulate climate-carbon cycle feedbacks: Results from an atmosphere-ocean general circulation model, *Biogeosciences*, *6*, 2099–2120.

Wigley, T. M. L. (2006), A combined mitigation/geoengineering approach to climate stabilization, *Science*, *314*, 452–454, doi:10.1126/science.